Luminosity measurement at BESIII*

November 13, 2006

Abstract

Measurement of luminosity at BESIII is discussed by virtue of theoretical estimation and previous experiences. Some Monte Carlo simulations are also performed for event selection and uncertainty estimation.

1 Introduction

High luminosity accelerator, CESR/CLEO-c, has been taken data in charmonium energy region. Another accelerator BEPC/BES is upgrating their accelerator to run at charmonium energy region with high luminosity. The optimized instant luminosity of these existent or will-be accelerator is up to 1×10^{32} or 1×10^{33} cm^2 s^{-1}. Total number of event collected by these accelerators is or will be at order of few fb^{-1}. Utilizing these large data samples, many physical analysis could be preformed with unprecedented precision.

In such accurate analysis, many meticulous factors and effects have to considered seriously. The first elementary and important analysis is about the luminosity itself, which is an important index for both detector and accelerator. As to the absolute measurement, such as τ mass measurement, R value measurement, J/ψ, ψ' or ψ'' scan measurement, luminosity is indispensable and its error will directly pass over to measured variable, say the cross section. The accuracy of luminosity play a key role in the error determination of the final results.

In e^+e^- colliding beam experiment, the generic physics analysis commonly requires the relative luminosity in data taken on and off the resonance so that backgrounds from continuum production may be accurately subtracted. Sometimes, an analysis will make an internal consistency check by dividing the dataset into independent subsets of comparable size, again relying on accuracy and stability of the relative luminosity. In addition, as the event used to calculate the luminosity, such as e^+e^-, $\mu^+\mu^-$ and $\gamma\gamma$, have salient topologies which can be used as online event monitor, moreover, the variation of cross section of the processes can be used to monitor the stability of accelerator and detector.

*Author: X.H.Mo, C.D.Fu, K.L.He

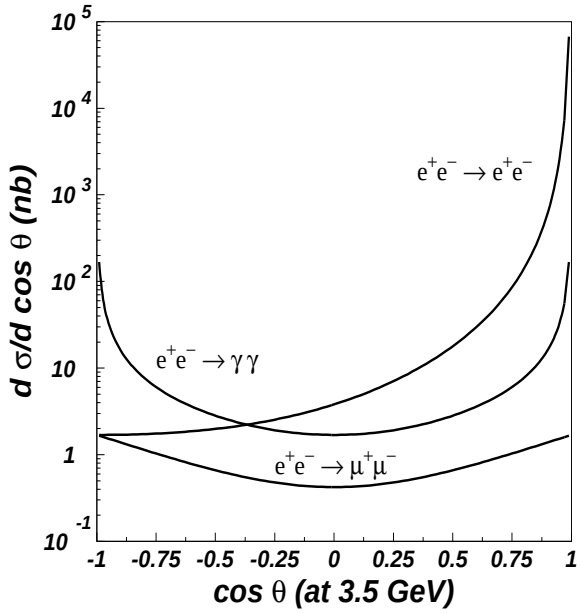

Figure 1: $d\sigma/d\cos\theta$ versus $\cos\theta$ distribution for three QED processes: $e^+e^- \to e^+e^-$, $e^+e^- \to \mu^+\mu^-$, and $e^+e^- \to \gamma\gamma$. The energy point is at 3.5 GeV.

Experimentally, there are two approaches to measure the luminosity, online approach and offline approach. The advantage for online measurement is mainly due to high count, fast trigger, to can be used as online monitor; the disadvantage lie in online measurement has the different dead-time from the offline data, and generally the uncertainty of online measurement is comparatively large. Conversely, the disadvantage for offline measurement is low count, slow identification but the advantage of offline measured luminosity has the same dead-time with the offline data and this is especially suitable for physics analysis. So in the following study, we only discuss about offline luminosity measurement.

In principle any process can be used for luminosity measurement, however in order to obtain precision results, one often select the process which has salient topology character experimentally and has accurate theoretical calculation of cross section. From these point of view, the QED processes such as $e^+e^- \to e^+e^-$, $e^+e^- \to \mu^+\mu^-$, and $e^+e^- \to \gamma\gamma$, are often adopted for luminosity measurement. The $d\sigma/d\cos\theta$ distribution these are show in Fig. 1, which are drawn by virtue of the following formulas:

$$\left.\frac{d\sigma}{d\Omega}\right|_{e^+e^-\to e^+e^-} = \frac{\alpha^2}{4s}\left(\frac{3+\cos^2\theta}{1-\cos^2\theta}\right)^2$$

$$\left.\frac{d\sigma}{d\Omega}\right|_{e^+e^-\to \mu^+\mu^-} = \frac{\alpha^2}{4s}\left(1+\cos^2\theta\right)$$

$$\left.\frac{d\sigma}{d\Omega}\right|_{e^+e^-\to \gamma\gamma} = \frac{\alpha^2}{4s}\left(\frac{1+\cos^2\theta}{(E_b/p)^2-\cos^2\theta}\right)^2$$

High accuracy is expected for forthcoming BESIII physics analysis and it is not an easy task even for the simple and elementary processes, such as e^+e^-, $\mu^+\mu^-$ and $\gamma\gamma$. To minimize both theoretical and systematic uncertainties, the recommendable approach is to separately analyze three different processes which have large and well-known cross section: final state pairs of electrons, muons and photons. Experimentally, the response of the detector to each of these reactions is quite distinct: efficiencies rely on charged particle tracking (e^+e^-), calorimetry (e^+e^- and $\gamma\gamma$), muon counter ($\mu^+\mu^-$), and triggering in different ways for each process. The expected theoretical cross sections are calculable in quantum electrodynamics; weak interaction effects are negligible. The primary theoretical obstacle in all cases is computation of the electromagnetic radiative corrections in a way that accommodates experimental event selection criteria and achieves adequate precision. This is usually accomplished with a Monte Carlo event generator which properly includes diagrams with a varying number of virtual and real radiative photons to consistent order in α. Of course, more accurate theoretical calculations are appreciate which could lead to smaller uncertainty.

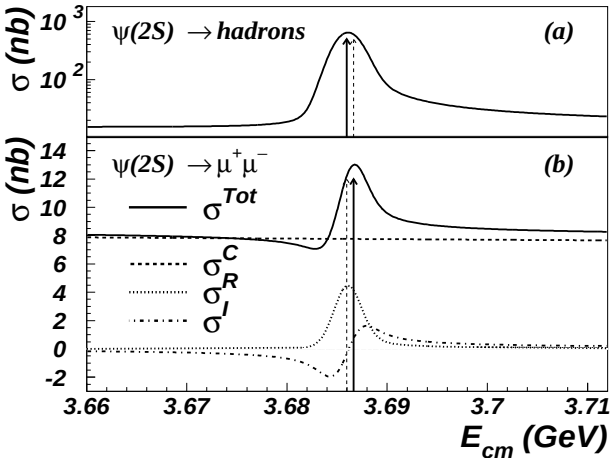

Figure 2: Cross sections in the vicinity of $\psi(2S)$ for inclusive hadrons (a) and $\mu^+\mu^-$ (b) final states. The solid line with arrow indicates the peak position and the dashed line with arrow the position of the other peak. In (b), dashed line for QED continuum (σ^C), dotted line for resonance (σ^R), dash dotted line for interference(σ^I), and solid line for total cross section(σ^{Tot}).

Another factor which can not be neglected is the interference effect in the vicinity of resonance peak. Such an effect not only distort the cross section in the peak region but also shift the maximum position of the resonance peak as shown in Fig. 2 as an example. The section ratios between resonance and continuum at J/ψ, ψ', and ψ'' regions are listed in Table 1, by virtue of which we can see at continuum region all there processes can be used to calculate the luminosity while at resonance region, all there processes can be adopted for ψ'', only two of them ($\gamma\gamma$ and e^+e^- can be adopted for ψ', as to J/ψ

merely $e^+e^- \to \gamma\gamma$ process is suitable for luminosity measurement if fairly high accuracy is required.

Table 1: Section ratios between resonance and continuum at J/ψ, ψ', and ψ'' regions.

Res./Con.	J/ψ	ψ'	ψ''
$\mu^+\mu^-$	15.3	0.625	$< 1.28 \times 10^{-5}$
e^+e^-	0.700	0.027	6.0×10^{-5}
$\gamma\gamma$	$< 6 \times 10^{-3}$	$< 5.8 \times 10^{-3}$	$< 5.8 \times 10^{-3}$

2 Event selection and Algorithm

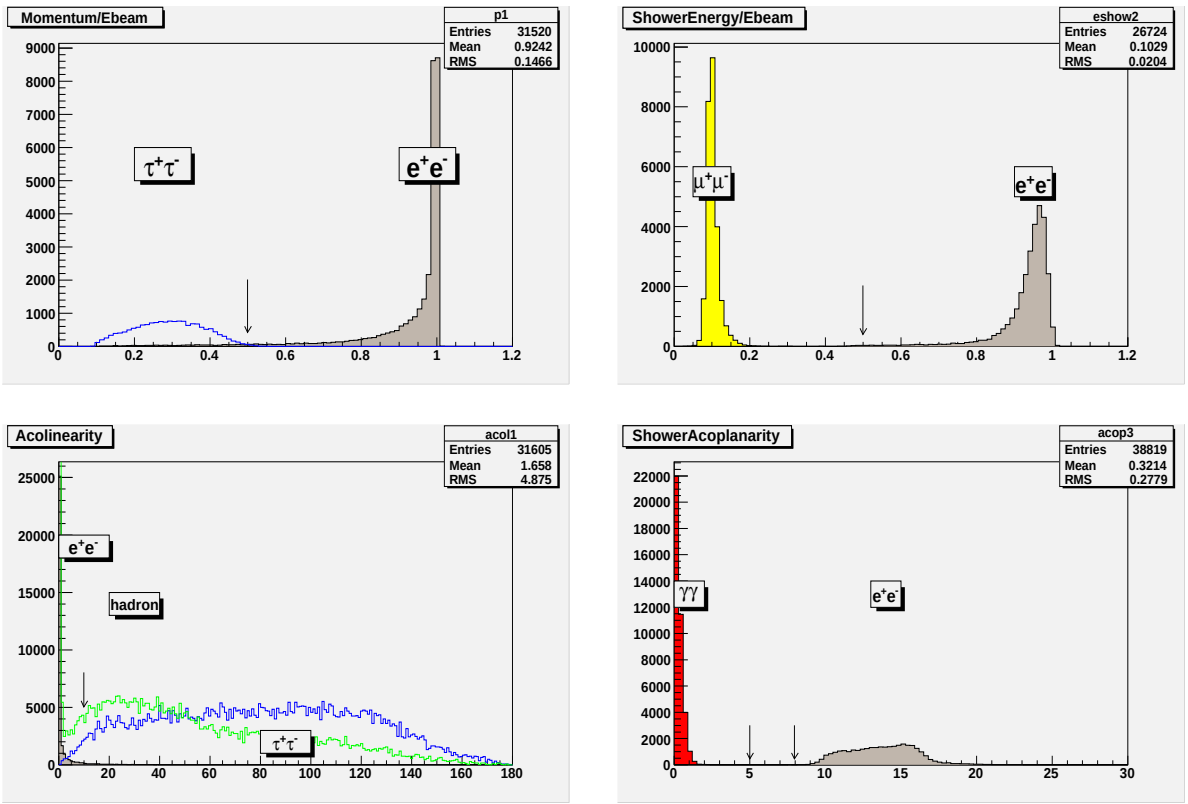

Figure 3: Some special distributions for event selection, including momentum, energy deposit, acollinearity, and acoplanarity. Usually two samples with distinctive feature are drawn in the same plot, and the corresponding variable can be used to select one sample and veto another at the same time.

To determine the event selection criteria, a variety of distributions for track information should be scrutinized, from which some special information variables are selected to distinguish one kind of event from the others. Some typical distributions for event

selection, such as momentum (normalized by beam energy), energy deposit (normalized by beam energy), acollinearity (constructed by momenta measured in MDC), and acoplanarity (constructed by information of EMC), are displayed in Fig. 3. Two samples with distinctive feature are drawn in the same plot, and the corresponding variable can be used to select one sample and veto another at the same time.

The even selection criteria for e^+e^-, $\gamma\gamma$, and $\mu^+\mu^-$ final states are tabulated in Table 2. Anyway, due to various hard-ware and soft-ware problems, more studies are need and further improvement is possible and necessary.

Table 2: Selection criteria for e^+e^-, $\gamma\gamma$, and $\mu^+\mu^-$ final states.

Description	e^+e^-	$\gamma\gamma$	$\mu^+\mu^-$
# neutral tracks		≥ 2	
# charged tracks	≥ 2 ($< n$, n decided by detector state)	≤ 1?	=2
$\lvert\cos\theta\rvert$	< 0.8	< 0.8	< 0.8
Track momentum	$> 0.5E_b$		(0.5-1.15)E_b
Track acollinearity	$< 10^\circ$		$< 10^\circ$
$\cos\theta_1 \times \cos\theta_2$	< 0.02	< 0.001	< 0
Shower Energy	(0.5-1.1)E_b	$> 0.5E_b$	(0.1-0.35) GeV
Shower acoplanarity	$> 8^\circ$	$< 2^\circ$	$> 5^\circ$
Vertex & TOF			$\lvert t1 - t2\rvert < 3$ ns

3 Systematic uncertainty

Some typical luminosity measurement results are adduced in Table 3, according to which the uncertainty for luminosity measurement at BES is around 2-3 %. Some comparatively high accurate results from other experiment group are collected in Table 4. For the forthcoming new detector, the uncertainty is expected to be around 1%.

To achieve the 1% accuracy, effects on many aspects should be taken into account, which include

1. Backgrounds analysis;
2. Trigger efficiency;
3. Error due to Monte Carlo simulation;
4. Stability of data taking;

Table 3: Uncertainty of Luminosity from measurement of e^+e^- final state at BES. The online luminosity is measured by small angle luminosity monitor while offline luminosity is measured by large angle Bhabha event.

Energy region	J/ψ	ψ'	ψ''	R-value
Method	online	offline	offline	offline
Uncertainty	6%	3.2%	1.83%	$< 3\%$
Reference	[1]	[1]	[3]	[4]

Table 4: Error of Luminosity from other experiments

Exp. Group	$E_{c.m.}$	Mode	Error	Ref.
CLEO	10 GeV	e^+e^-, $\mu^+\mu^-$, $\gamma\gamma$	1.0%	[5]
DAΦNE	1-3 GeV	e^+e^-	0.6%	[6]

5. Theoretical accuracy, mainly about the radiative correction.

We will discuss all relevant factors one by one in the following subsections. Since the real data is unavailable for the time being, our systematic study is performed merely in the light of previous BESII analysis, experience from other experiment groups, especially CLEOc collaboration, whose detector is similar to the BESIII detector in many aspects.

3.1 Background analysis

We copy the background analysis in Ref. [5] *verbatim et litteratim*, since most of the part can similarly or directly used in the future BESIII ananlyses.

Cosmic rays dominate the background in the μ-pair sample. Tight track quality requirements minimize this contamination with almost no loss in efficiency. The remaining cosmic background is estimated with two independent variables, impact parameter (denoted as $d_\pm$ for positive or negative charge), which indicate the distance of closest approach to the beam-axis in the plane transverse to the beam) and time-of-fight (TF). For the first method, the distribution of μ^- impact parameter d_- is compared with that from a relatively pure sample of cosmic rays. To obtain the cosmic ray sample, a variable based on TF is required to be inconsistent with the event originating as an e^+e^-; interaction: $T = \sqrt{t_+^2 + t_-^2} > 4$ ns, where $t_+(t_-)$ is the time recorded by the TF counter struck by the $\mu^+(\mu^-)$; relative to the expected time. Fig. 4(a) shows d_- on events for which the impact parameter requirement has been loosened from 1.5 mm to 3.0 mm overlaid with that of the cosmic sample, which has been normalized in the tail region $|d_-| > 2$ mm. The small enhancement near zero in the cosmic ray curve is due to the presence of true

μ-pairs in this subsample from TF mismeasurement. Accounting for this effect, the fraction of cosmic rays with $|d_-| < 1.5$ mm is $(0.5 \pm 0.1)\%$. For the time-of-flight method, the fraction μ-pairs that have $T > 4$ ns (see Fig. 4(b)) is $(0.6 \pm 0.1)\%$, in good agreement with the impact parameter method. Background from τ-pair decays, according to the KORALB [7] Monte Carlo, is 0.07%, and from $e^+e^-\mu^+\mu^-$ events [8] is $< 0.002\%$.

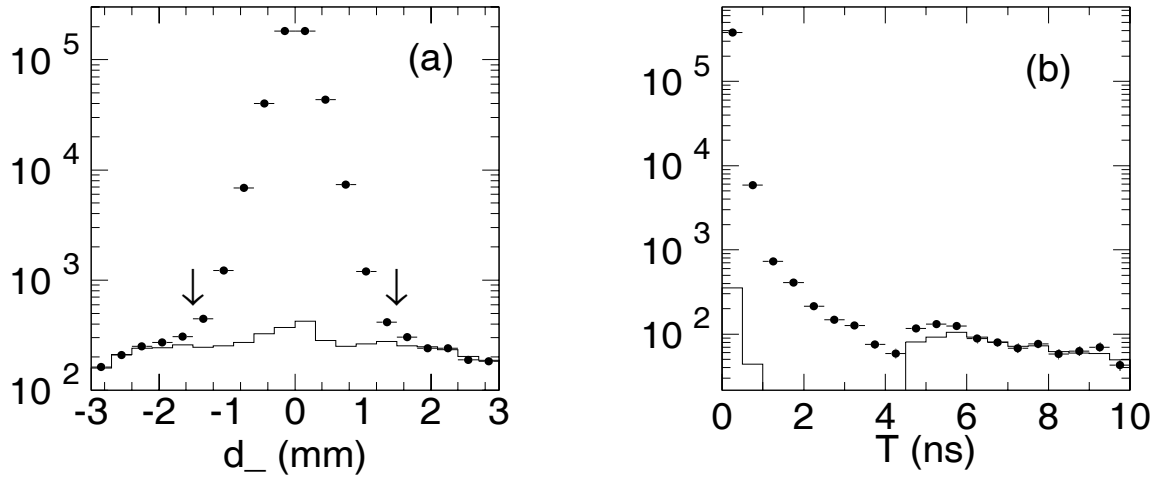

Figure 4: Distribution on μ-pair and cosmic ray events of (a) impact parameter for the negative track d_-, and (b) time-of-flight variable T. In (a) the data are shown with the $d_\pm$ cut relaxed (solid circles); cosmic rays are selected with $T > 4$ ns (histogram) and normalized for $|d_-| > 2$ mm. The arrows indicate the default requirement $d_\pm < 1.5$ mm. In (b), cosmic rays (histogram) are selected with $d_- > 2$ mm and normalized for $T > 6$ ns.

The background in photon pair events from Bhabhas that have no tracks (because they do not fire an L0 TF trigger) can be easily estimated. The product of the probability for a Bhabha to have no tracks ($\sim 0.8\%$), the probability for a Bhabha to satisfy all the criteria *except* zero or one track ($\sim 1.5\%$), and the ratio of the Bhabha to $\gamma\gamma$ acceptance yields a relative background of $(0.1 \pm 0.1)\%$. There is no evidence for any other signicant backgrounds in the sample.

For Bhabhas, τ-pairs contribute 0.03% background. A Monte Carlo generator [9] for the final state $e^+e^-e^+e^-$ yields an estimate of $(0.05 \pm 0.05)\%$ background. The level of cosmic rays in the sample can be estimated in three ways, two of which are similar to the techniques used for μ-pairs. The time-of-flight variable T and the tails of the track impact parameter distribution show no evidence of cosmic rays. Only 0.05% of all events have one reconstructed muon track penetrating the first layer of magnet iron, and only 0.0015% have two, indicating the level of cosmic rays must be small. The total background in e^+e^- events is assumed to be $(0.1 \pm 0.1)\%$.

The background estimated by CLEOc for all three kinds of background is at the level of 0.1%, which is expected at BESIII. Anyway, due to difference of detector and simulation system, such an estimation may no be conservative and considerable effects should be made to reach such an precision.

3.2 Trigger efficiency

The trigger [10] of BES is implemented through a trigger table which includes 8 channels and 15 conditions for each channel. The logic relation between conditions is "and" that means the trigger efficiency of a channel is the product of several trigger conditions used, while the logic relation among channels is "or" that means the events would be recordered if they satisfy any channel trigger. A special trigger table, as adduced in Table 5, is used to study the trigger efficiency for peculiar subdetector and trigger condition. In fact each condition is related with BES different subdetectors' information or event topology, the concrete information has been given in table 6. More details for evaluating the trigger efficiency can be found in Ref. [11].

In practice, a carefully studied trigger table is adopted for certain physics aim. As an example, presented in table 7 is the one used for ψ' scan. Totally 4 channels and 10 trigger conditions were set for the actual data taking.

Table 8 provide the trigger efficiencies for ψ' scan and R-value measurement. As claimed in Ref. [13], the error of trigger efficiency is less than 0.5%. Comparing with CLEO results, as adduced in Table 8, the method once adopted by BESII is good enough to provide accurate trigger efficiency, especially for $\mu^+\mu^-$ final state. The similar method is expected to also adopted at BESIII, so the uncertainty due trigger efficiency is estimated at the level of 0.5%.

3.3 Monte Carlo simulation

The uncertainty due to Monte Carlo simulation can be analyzed by comparing the data distributions with those corresponding ones from simulation. Shown in Fig. 5 are typical comparing distributions on Bhabha and $\gamma\gamma$ events according to CLEOc analyses [5]. So far as uncertainties are concerned, differences between data and Monte Carlo are quantified by assigning systematic errors to the acceptance which accommodate changes induced by reasonable variations in all the selection criteria. This procedure results in errors attributed to inadequate detector modeling of 1.1%, 0.9%, and 1.4respectively.

Anyway, the above estimation from CLEOc is not very favorable. Since the so-called "reasonable variations in all the selection criteria" sounds rather ambiguous and lack of operativeness. Comparatively, the method provided in Ref. [6] is fairly practical.

As shown in Fig. 6, the possible uncertainty due to polar angle selection is mainly

Table 5: Trigger condition table for trigger study

Channel	MDC	VC	BSC	TOF	ESC	ETOF	ENDVC	MUON
Active?	Y	Y	Y	Y	Y	Y	Y	Y
TOF BB	-	-	Y	-	-	-	-	Y
$Ntof \geq 1$	-	-	-	-	-	-	-	-
$Ntof \geq 2$	Y	Y	-	-	-	-	-	-
Radial	-	-	-	-	-	-	-	-
$Nvc \geq 1$	Y	-	Y	Y	Y	Y	-	-
$Netof \geq 1$	-	-	-	-	-	-	-	-
ETOF B-B	-	-	-	-	Y	-	Y	-
$Ntrk \geq 1$	-	-	-	-	-	-	-	Y
$Ntrk \geq 2$	-	Y	Y	Y	-	-	-	-
$Ntrk \geq 4$	-	-	-	-	-	-	-	-
Eradial	-	-	-	-	-	-	-	-
ESC-Etot	-	-	-	-	-	Y	Y	-
Etot.l	Y	Y	-	Y	-	-	-	-
Etot.h	-	-	-	-	-	-	-	-

Note: the row beginning with " **active ?**" indicates which channels will be used or not, denoting by "Y" or "N".

Table 6: Sub-detectors and Trigger conditions

relevant sub-detector	trigger conditions and their meanings
MDC (Main Drift Chamber)	$Ntrk \geq 1, Ntrk \geq 2, Ntrk \geq 4$ (at least 1,2 or 4 tracks in MDC found by trigger tracking system
TOF (Time of Flight)	$TOFB-B$ (back-to-back hits found in TOF) $Ntof \geq 1, Ntof \geq 2$ (at least 1 or 2 hits found in TOF)
ETOF (Endcap Time of Flight)	$ETOFB-B$ (back-to-back hits found in ETOF)
BSC (Barrel Shower Chamber)	$RADIAL$ (total radial energy deposited in BSC) $Etot.l, Etot.h$ (low or high threshold of energy deposited in BSC)
ESC (Endcap Shower Chamber)	$Eradial$ (total radial energy deposited in ESC) $ESCEtot$ (low threshold of energy deposited in ESC)
VC (Vertex Chamber)	$Nvc \geq 1$ (at least 1track found in VC)

Table 7: Trigger condition table for ψ' scan

Channel Condition	BHAHBA	CHARGED	2-MU	CHAR2	NEUTRAL	Eneutral	ESC	BB2
Active?	N	Y	N	Y	Y	N	Y	N
$TOFBB$	-	-	Y	-	-	-	-	Y
$Ntof \geq 1$	-	Y	Y	-	-	-	-	-
$Ntof \geq 2$	-	-	-	Y	-	-	-	Y
$RADIAL$	-	-	-	-	Y	-	-	-
$Nvc \geq 1$	-	Y	Y	Y	-	Y	Y	-
$Eradial$	Y	-	-	-	-	-	-	-
$ETOFBB$	-	-	-	-	-	-	Y	-
$Ntrk \geq 1$	-	Y	-	-	-	-	-	Y
$Ntrk \geq 2$	-	-	-	Y	-	-	-	-
$Ntrk \geq 4$	-	-	-	-	-	-	-	-
$Etrk$	-	-	-	-	-	Y	-	-
$ESC - Etot$	-	-	-	-	-	-	Y	-
$Etot.l$	-	Y	-	-	-	-	-	Y
$Etot.h$	-	-	-	-	Y	-	-	-

Table 8: Trigger Efficiencies of ψ' scan and R-value measurement at BES and of luminosity measurement at CLEO. R.E. is short for relative error.

BES Trigger Efficiency				
Physics	e^+e^-	$\mu^+\mu^-$	$hadron$	Reference
ψ' scan	0.99998	0.99361	0.99847	[12]
R-value scan	0.999626	0.993267	0.997632	[13]
CELO Trigger Efficiency				
Process	e^+e^-	$\mu^+\mu^-$	$\gamma\gamma$	Reference
Efficiency (%)	98.9 ± 0.5	99.7 ± 0.1	85.3 ± 1.1	[5]
R.E. (%)	0.5	0.1	1.3	

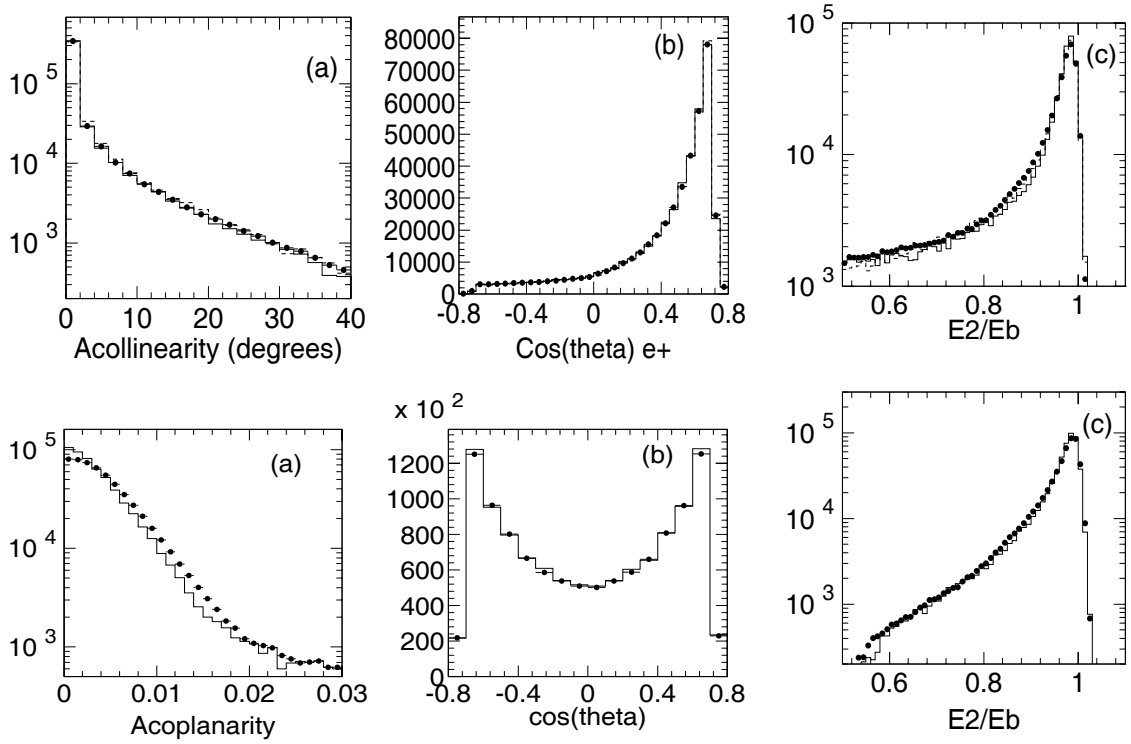

Figure 5: Up-distributions on Bhabha events for data (solid circles), BHLUMI Monte Carlo (solid histogram) and BK*ee* Monte Carlo (dashed histogram) in (a) acollinearity of the two tracks; (b) $\cos\theta$ of the positron; (c) the smaller of (a) and (b) shower energies, scaled to the beam energy. Down-distributions on $\gamma\gamma$ events for data (solid circles), and BK$\gamma\gamma$ Monte Carlo (solid histogram) in (a) shower acoplanarity; (b) $\cos\theta$ of the positron; (c) the energy of the second highest energy photon, scaled to the beam energy. [all figures from Ref. [5]]

from the border region. To evaluate such effect, the relative difference between data and Monte Carlo is computed in the border intervals ($55^\circ < \theta < 65^\circ$, $115^\circ < \theta < 125^\circ$), after normalizing the number of Monte Carlo events, N_{MC}, to coincide with the number of data events, N_{data}, in the central region ($65^\circ < \theta < 115^\circ$): the value $(N_{data} - N_{MC})/N_{data} = (-0.25 \pm 0.03)\%$ is used both as the relative correction to the effective cross section and as systematic uncertainty on the angular acceptance. This estimate is confirmed by computing the relative variation of the luminosity as a function of the value of the cut in polar angle, θ_{cut}:

$$\begin{aligned} \frac{\Delta\mathcal{L}}{\mathcal{L}} &= \frac{N_{\rm VLAB}(\theta_{\rm cut} < \theta < 180^\circ - \theta_{\rm cut})}{N_{\rm VLAB}(55^\circ < \theta < 125^\circ)} \\ &- \frac{\sigma_{\rm eff}(\theta_{\rm cut} < \theta < 180^\circ - \theta_{\rm cut})}{\sigma_{\rm eff}(55^\circ < \theta < 125^\circ)} \end{aligned}$$

The behaviour of $\Delta\mathcal{L}/\mathcal{L}$ as a function of $\theta_{\rm cut}$ shows that, in a 5° range, the relative variation is $\Delta\mathcal{L}/\mathcal{L} = ^{+0.003}_{-0.002}$, consistent with the quoted systematic error.

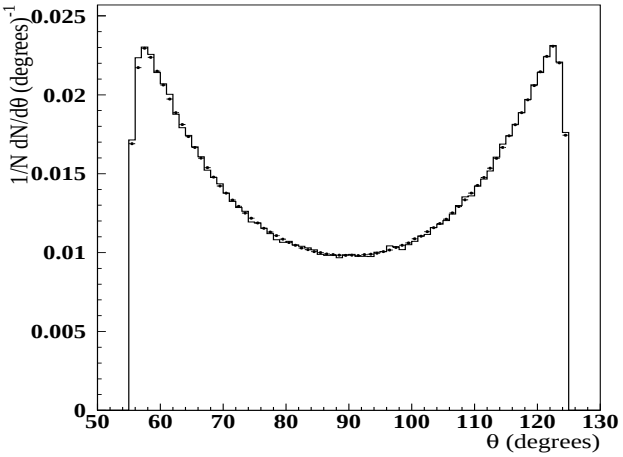

Figure 6: Comparison between the data (points) and Monte Carlo (histogram) distributions of energy clusters polar angle normalized to the same number of events.

3.4 Stability

Since the environment of detector keep changing over running time, although the online calibration smooths some fluctuations on large extent, some variations may still survive. Therefore it is necessary to check the stability of luminosity measurement, that is the variation of luminosity with the running time.

For CLEOc, the time dependence of the $\gamma\gamma$ or μ-pair to Bhabha luminosity ratio in bins of $\sim$ 40pb^{-1} or $\sim$ 125pb^{-1} is shown in Fig. 7(a) or (b), respectively; both with statistical error only. Both ratios are quite stable:

$$\mathcal{L}(\gamma\gamma)/\mathcal{L}(e^+e^-) = 0.990 \pm 0.001 \ ,$$

and

$$\mathcal{L}(\mu^+\mu^-)/\mathcal{L}(e^+e^-) = 0.997 \pm 0.002 \ .$$

Using the statistical errors, the χ^2 for ratios to be constant are 57 for 56 d.o.f and 75 for 18 d.o.f, respectively. Hence there are no time dependent systematic effects for $\gamma\gamma$'s and Bhabhas, but the μ-pair statistical errors need to be doubled to bring the χ^2/d.o.f down to unity. Anyway, the uncertainty due to stability is negligible in CLEOc luminosity measurement.

For DAΦne, the stability is also checked. As example, shown in Fig. 8 are distributions of the cluster energy of VLAB events for three runs (points), one from each of the three different periods of data taking, compared with Monte Carlo (solid line). The analysis

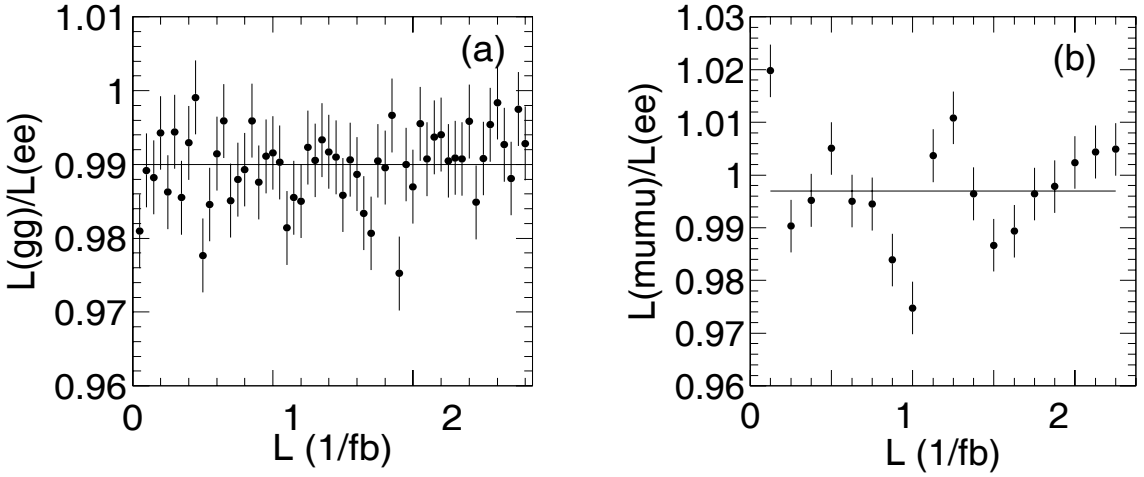

Figure 7: Ratio of different measures of luminosity as a function of integrated luminosity: (a) $\mathcal{L}(\gamma\gamma)/\mathcal{L}(e^+e^-)$ in bins of $\sim 40\text{pb}^{-1}$; and (b) $\mathcal{L}(\mu^+\mu^-)/\mathcal{L}(e^+e^-)$ in bins of $\sim 125\text{pb}^{-1}$. (Fig.7 of Ref. [5])

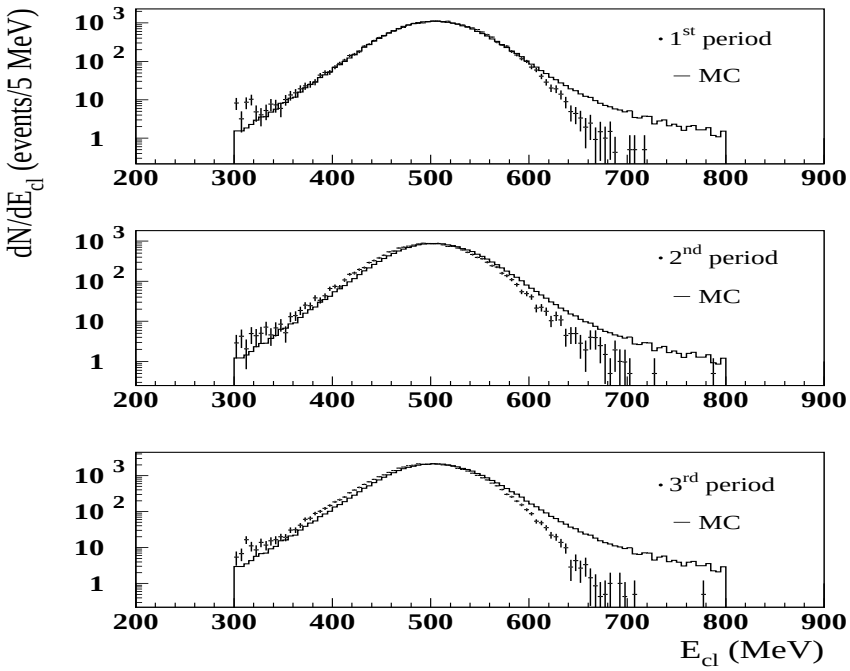

Figure 8: Distribution of the cluster energy of VLAB events for three runs (points), one from each of the three different periods of data taking, compared with Monte Carlo (solid line).(Fig.6 of Ref. [6])

indicate the uncertainty due to stability is at the level of 8.6×10^{-4} [6], which is also negligible for luminosity measurement.

For future luminosity measurement at BESIII, the stability is to be checked, and at present its uncertainty effect is not taken into account.

3.5 Theoretical accuracy

Theoretical accuracy is actually constraited by the accuracy of ISR calculation.

Table 9: Generator for e^+e^-, $\gamma\gamma$, and $\mu^+\mu^-$ final states.

Item	e^+e^-	$\gamma\gamma$	$\mu^+\mu^-$
CLEOc: cross section at Eb=5.29 GeV			
α^3 generator	BKee	BK$\gamma\gamma$	BKJ
cross section (nb)	8.45 ± 0.02	1.124 ± 0.002	0.429 ± 0.001
α^3 generator	BHLUMI		FPAIR
cross section (nb)	8.34 ± 0.02	–	0.427 ± 0.001
$\Delta(\alpha^4\&\alpha^3)$	-1.3%	$[-1.3\%]$	0.5%
BESII: suitable for any energy region			
α^3 generator	Radee	Radgg	Radmu
BESIII: suitable for any energy region			
KKMC			

For CLEOc analysis, in each case radiative photons are generated above some photon energy cutoff $k_0 = E_\gamma/E_b$, and all diagrams with softer photons are subsumed into the two body final state. Two generators each were used for e^+e^- and $\mu^+\mu^-$ scattering, and one for $\gamma\gamma$ events. The BKee program [14] generates e^+e^- final states with zero or one radiative photon yielding a cross section accurate to order-α^3. Higher order corrections are available in the BHLUMI program [15], which uses Yennie-Frautschi-Suura exponentiation to generate many photons per event and yields a cross section accurate to order-$\alpha^4 ln^2(|t)/m_e^2))$, where t is the typical momentum-transfer. As with BKee, the the BK$\gamma\gamma$ Monte Carlo [16] generates events with up to one radiative photon and yields an order-α^3 cross section, as does the BKJ generator [17] for μ-pairs. Up to three radiative photons in $\mu^+\mu^-$ events are possible (two from initial state radiation and one from final state radiation) with FPAIR [18], which has an order-α^4 accuracy. A photon cutoff of $k_0 = 0.01$ is used for BKee, BK$\gamma\gamma$, and BKJ, and $k_0 = 0.001$ for BHLUMI and FPAIR. The generators used in CLEOc analysis and the cross sections at $E_b = 5.29$ GeV are quoted in Table 9.

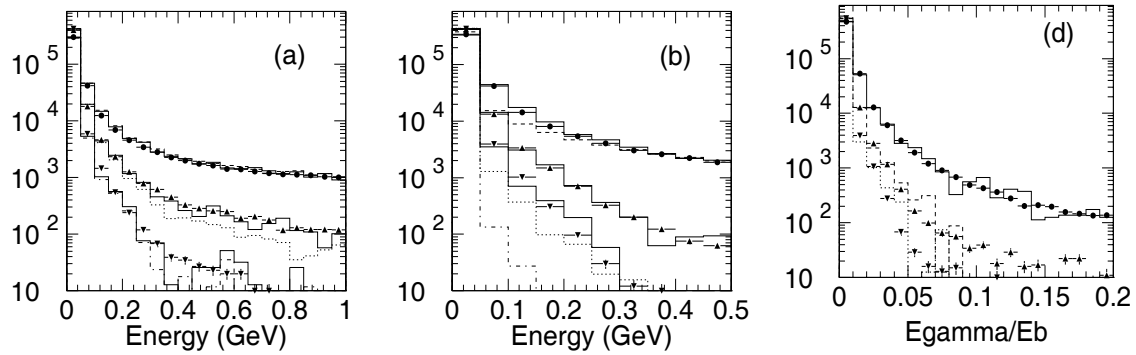

Figure 9: Distributions in the energy of the first, second and third most energetic photon per event for data (solid circles, upward- and downward-pointing triangles), α^4 Monte Carlo (solid histograms), and α^3 Monte Carlo (dashed, dotted, and dot-dashed histograms), respectively, for (a) e^+e^-, (b) $\mu^+\mu^-$ and (d) $\gamma\gamma$ events. [all figures from Ref. [5]]

At BESII, only used are the generators with cross section accuracy up to order-α^3. At BESIII, a generic generator KKMC is to be adopted, which could provide cross section accuracy up to order-α^4. However, even the high accuracy generator is adopted, many cross checks are still indispensable to ensure the correctness of the algorithm. One check is to compare the multiphoton distribution between data and Monte Carlo. Shown in Fig. 9 are comparison of distributions in the energy of the first, second and third most energetic photon (besides the two charged tracks for e^+e^- and $\mu^+\mu^-$ or two neutral tracks for $\gamma\gamma$) per event. Consistence will reflect the reliability of theoretical calculation and corresponding Monte Carlo simulation.

Another kind of check to ensure the correctness of theoretical calculation is to compare the results from different kinds of generator simulations. For DAΦNE analysis, the event generators `Babayaga` [19, 20] and `Bhagenf` [21], developed for the large angle Bhabha scattering based on the cross section calculated in [14], have been interfaced with the detector simulation program `GEANFI` [22] for evaluating the effective cross section, as well as for estimating the systematic uncertainties. After applying the `VLAB` selection we find an agreement better than 0.1% between the cross sections calculated with the two generators, including the event reconstruction efficiency:

$$\texttt{Babayaga} \quad \sigma_{\rm eff} = (431.0 \pm 0.3)\ \text{nb}$$

$$\texttt{Bhagenf} \quad \sigma_{\rm eff} = (430.7 \pm 0.3)\ \text{nb}$$

The error given in the above cross section is due to the Monte Carlo statistics. The systematic theoretical uncertainty claimed by the authors is 0.5% in both cases. The radiative corrections due to the treatment of initial and final state radiation in `Bhagenf` and `Babayaga` have been compared with two other event generators: the `Bhwide` code [23]

developed for LEP and the `Mcgpj` code [24] developed for VEPP-2M and based on the cross section calculated in [25]. Further details on the event generators and the application in the analysis can be found in reference [26]. For this comparison, DAΦNE people applied the kinematic `VLAB` requirements on the generated momenta and computed the `VLAB` cross sections for the four generators, as shown in the table below, where errors are due to Monte Carlo statistics.

MC code	σ (nb)
`Bhagenf`	460.8 ± 0.1
`Babayaga`	459.4 ± 0.1
`Mcgpj`	457.4 ± 0.1
`Bhwide`	456.2 ± 0.1

These values are obtained without considering detector smearing and loss effects and therefore the results are considerably different from the effective `VLAB` cross section presented before, where a full detector simulation was performed. Moreover, contributions from the ϕ decay and vacuum polarization effects are not applied, because they are the same for all generators.

The agreement among the four generators supports the systematic uncertainty of 0.5% quoted by the authors of `Bhagenf` and `Babayaga`.

4 Summary

Table 10 summarizes the sources of error in the luminosity measurement at CLEO [5]. Comparatively speaking, some possible improvements at BESIII include

- Statistic : the 0.2% statistic uncertainty corresponds to 250,000 Monte Carlo event, therefore 1,000,000 event will accommodate the statistic uncertainty at level of 0.1%, which is easily realized at BESIII.
- Background : we expect the same level of background as CLEO, that is 0.1%;
- Trigger efficiency : as we mentioned in section 3.2, using trigger table, the uncertainty due to trigger efficiency is less than 0.5%;
- Consistency between data and Monte Carlo: 1.0 % ;
- Radiative correction : 1.0%.

With these estimations, the uncertainties of luminosity measurement at the forthcoming detector BESIII are listed in the Table 10, the final combined uncertainty is around 0.9%.

Table 10: Relative Error (%) in luminosity for CLEO and BESIII.

Exp.Group	CLEO			BES		
Source	e^+e^-	$\gamma\gamma$	$\mu^+\mu^-$	e^+e^-	$\gamma\gamma$	$\mu^+\mu^-$
Monte Carlo Statistic	0. 2	0. 2	0. 2	0. 2	0. 2	0. 2
Backgrounds	0. 1	0. 1	0. 1	0. 1	0. 1	0. 1
Trigger Efficiency	0. 5	0. 1	1. 3	0. 5	0. 1	1. 3
Detector Modeling	1. 1	0. 9	1. 4	1. 1	0. 9	1. 4
Radiative Corrections	1. 3	1. 3	1. 0	1. 3	1. 3	1. 0
Summed in Quadrature	1. 8	1. 6	2. 2	1. 8	1. 6	2. 2
combine	1.1%			0.9%		

References

[1] BES Collaboration, J.Z. Bai *et al.*, Phys. Lett. B **355**, 374 (1995); HEP & NP **19**, 673 (1995).

[2] BES Collaboration, J.Z. Bai *et al.*, Phys. Lett. B **550**, 24 (2002).

[3] BES Collaboration, M. Ablikim *et al.*, hep-ex/0605107.

[4] BES Collaboration, J.Z. Bai *et al.*, Phys. Rev. Lett. **84**, 594 (2000); Phys. Rev. Lett. **88**, 101802 (2002).

[5] CLEO Collaboration, G. Crawford *et al.*, CLNS 94/1268 (Jan. 27th, 1994).

[6] KLOE Collaboration, F. Ambrosino *et al.*, hep-ex/0604048.

[7] S. Jadach and Z. Was, Comp. Phys. Comm. 36 (1985) 191; S. Jadach and Z. Was, Comp. Phys. Comm. 64 (1991) 267; S. Jadach, J.H. Kuhn and Z. Was, Comp. Phys. Comm. 64 (1991) 275; M. Jezabek, Z. Was, S. Jadach and J.H. Kuhn CERN-TH-6195-91 (Aug. 1991).

[8] V.M. Budnev *et al.*, Phys. Rep. C15 (1975) 181.

[9] J. Vermasseren, Nucl. Phys. B299 (1993) 347.

[10] Y.N. Guo *et al.*, HEP & NP **14**, 1057 (1990) (in Chinese);
Z.Q. Yu *et al.*, HEP & NP **19**, 1062 (1995) (in Chinese).

[11] G.S. Huang *et al.*, HEP & NP **25**, 889 (2001).

[12] X.H. Mo, Measurement of $\psi(2S)$ resonance parameters, Ph.D. Thesis, Institute of High Eneregy Physics (IHEP), (2001, in Chinese).

[13] G.S. Huang, R-value measurement from 2.6 to 5 GeV, Ph.D. Thesis, Institute of High Eneregy Physics (IHEP), (1999, in Chinese).

[14] F. Berends and R. Kleiss, Nucl.Phys. B228 (1983) 537.

[15] S. Jadach, E. Richter-Was, B.F.L Ward and Z. Was, CERN-TH-6230-91 (Sept. 1991); S. Jadach, E. Richter-Was, B.F.L Ward and Z. Was, Phys. Lett. B268 (1991) 253; S. Jadach, and B.F.L Ward, Phys. Rev. D40 (1989) 3582; S. Jadach, E. Richter-Was, B.F.L Ward and Z. Was, Phys. Lett. B260 (1991) 438; S. Jadach, E. Richter-Was, B.F.L Ward and Z. Was, Phys. Lett. B253 (1991) 469; Version 1.22 was obtained from B. Ward for the application at CLEOc.

[16] F. Berends and R. Kleiss, Nucl.Phys. B186 (1981) 22.

[17] F. Berends, R. Kleiss and S. Jadach, Nucl.Phys. B202 (1982) 63.

[18] F. Berends a nd S. van der Mark, Nucl.Phys. B342 (1990) 61.

[19] C.M. Carloni Calame *et al.*, Nucl. Phys. B **584** (2000) 459.

[20] C. M. Carloni Calame, Phys. Lett. B **520** (2001) 16.

[21] E. Drago and G. Venanzoni, "A Bhabha generator for DAΦNE including radiative corrections and Φ resonance", report INFN-AE-97-48.

[22] F. Ambrosino *et al.* [KLOE Coll.], Nucl. Instrum. Meth. A **534** (2004) 403.

[23] S. Jadach, W. Placzek and B.F.L. Ward, Phys. Lett. B **390**(1997) 298.

[24] G.V. Fedotovich and A.L. Sibidanov, Nucl. Phys. B(Proc. Suppl.) **131** (2004) 9.

[25] A. B. Arbuzov *et al.*, JHEP **9710** (1997) 001.

[26] A. Denig and F. Nguyen, "The KLOE luminosity measurement", KLOE note n.202, July 2005, `www.lnf.infn.it/kloe/pub/knote/kn202.ps`.